

## Article

# MoHG1 Regulates Fungal Development and Virulence in *Magnaporthe oryzae*

Xin Pu <sup>1,2,†</sup>, Aijia Lin <sup>1,2,†</sup>, Chun Wang <sup>1,2</sup>, Sauban Musa Jibril <sup>1,2</sup>, Xinyun Yang <sup>1,2</sup>, Kexin Yang <sup>1,2</sup>, Chengyun Li <sup>1,2,\*</sup> and Yi Wang <sup>1,2,\*</sup>

<sup>1</sup> State Key Laboratory for Conservation and Utilization of Bio-Resources in Yunnan, Yunnan Agricultural University, Kunming 650201, China; puxin\_1998@163.com (X.P.); laj7411@126.com (A.L.); chunwang775@gmail.com (C.W.); saubanzango@gmail.com (S.M.J.); yang-xinyun2001@163.com (X.Y.); 18468006252@163.com (K.Y.)

<sup>2</sup> Yunnan-CABI Joint Laboratory for Integrated Prevention and Control of Transboundary Pests, Yunnan Agricultural University, Kunming 650201, China

\* Correspondence: licheng\_yun@163.com (C.L.); wyi\_0114@ynau.edu.cn (Y.W.)

† These authors contributed equally to this work.

**Abstract:** *Magnaporthe oryzae* causes rice blast disease, which threatens global rice production. The interaction between *M. oryzae* and rice is regarded as a classic model for studying the relationship between the pathogen and the host. In this study, we found a gene, *MoHG1*, regulating fungal development and virulence in *M. oryzae*. The  $\Delta$ *Mohg1* mutants showed more sensitivity to cell wall integrity stressors and their cell wall is more easily degraded by enzymes. Moreover, a decreased content of chitin but higher contents of arabinose, sorbitol, lactose, rhamnose, and xylitol were found in the  $\Delta$ *Mohg1* mutant. Combined with transcriptomic results, many genes in MAPK and sugar metabolism pathways are significantly regulated in the  $\Delta$ *Mohg1* mutant. A hexokinase gene, *MGG\_00623* was downregulated in  $\Delta$ *Mohg1*, according to transcriptome results. We overexpressed *MGG\_00623* in a  $\Delta$ *Mohg1* mutant. The results showed that fungal growth and chitin contents in *MGG\_00623*-overexpressing strains were restored significantly compared to the  $\Delta$ *Mohg1* mutant. Furthermore, *MoHG1* could interact with *MGG\_00623* directly through the yeast two-hybrid and BiFC. Overall, these results suggest that *MoHG1* coordinating with hexokinase regulates fungal development and virulence by affecting chitin contents and cell wall integrity in *M. oryzae*, which provides a reference for studying the functions of *MoHG1*-like genes.

**Keywords:** *MoHG1*; cell wall integrity; chitin; hexokinase; rice blast



**Citation:** Pu, X.; Lin, A.; Wang, C.; Jibril, S.M.; Yang, X.; Yang, K.; Li, C.; Wang, Y. *MoHG1* Regulates Fungal Development and Virulence in *Magnaporthe oryzae*. *J. Fungi* **2024**, *10*, 663. <https://doi.org/10.3390/jof10090663>

Academic Editor: Mahfuz Rahman

Received: 17 August 2024

Revised: 18 September 2024

Accepted: 18 September 2024

Published: 21 September 2024



**Copyright:** © 2024 by the authors. Licensee MDPI, Basel, Switzerland. This article is an open access article distributed under the terms and conditions of the Creative Commons Attribution (CC BY) license (<https://creativecommons.org/licenses/by/4.0/>).

## 1. Introduction

*Magnaporthe oryzae* causes rice blast disease, which threatens global rice production. The pathogen can infect various grass hosts besides rice [1,2]. Genomic analyses revealed that there might be 10 distinct *M. oryzae* lineages and isolates from each lineage only infect a single host [3]. Recently, the emergence of *M. oryzae* *Triticum* (*MoT*) has caused serious losses in wheat production. The newest finding underlined that *MoT* was generated from the cross progeny of *Eleusine*- and *Urochloa*-infecting isolates and underwent a series of matings with a small number of individuals from three additional host-specialized populations [4]. However, phylogenetic analyses indicated a distant relationship between rice- and wheat-infecting populations. Our previous results also found a stronger selective sweep in the rice-infecting population than in the wheat-infecting population [5]. Thus, explorations of host selection mechanisms by *M. oryzae* favor decreasing the pathogen risk.

The fungal cell wall is composed of two layers. The inner layer has a cross-linked chitin-glucan matrix, and the outer layer possesses mannosylated proteins [6]. Chitin is a core component of the fungal cell wall, and UDP-N-acetylglucosamine is the substrate for chitin synthesis. Chitin is also a key elicitor to trigger plant immune response. Chitin modification

in pathogens and recognition by the host are determinants of disease occurrence [7,8]. There are two effectors, MoChia1 and Slp1, which influence chitin modification and infection in *M. oryzae* [9,10]. Moreover, melanin is also found in the cell wall of numerous fungal pathogens, which mainly reinforces cell structure and maintains the pressure from appressorium [11,12]. So far, diverse chitin and melanin synthesis enzymes have been identified, most of which are essential for fungal development and infectious processes [7].

Carbon metabolism is essential for fungal cell wall development. Monosaccharides with glucosyl residues mainly take up 75% of monosaccharides of cell walls. Other monosaccharides are mannose (14%), N-acetylglucosamine (7%), galactose (2%), and traces of arabinose and xylose in *M. oryzae* [13]. The carbon catabolite repression (CCR) system is widely conserved in filamentous fungi and favors fungi to preferentially utilize a favorable carbon source [14]. In *M. oryzae*, Tps1 is responsible for glucose-6-phosphate sensing and triggers CCR via the inactivation of Nmr1-3 [15,16]. The CCR transcription factor MoCreA has been identified, which regulates the utilization of different carbon sources and gene expressions [17].

Many proteins on fungal cell walls preferentially perceive various cues from a host and regulate fungal infection. G-protein-coupled receptors Pth11 and WISH, hydrophobin proteins Mpg1 and Mhp1, transmembrane mucin Msb2, and membrane sensor MoSho1 were identified in *M. oryzae* [18–21]. These sensor proteins can transduce the signals for appressorium development in the of *M. oryzae*. Fungal cell wall integrity (CWI) proteins are essential for cell viability, morphogenesis, and pathogenesis. In *M. oryzae*, there are three mitogen-activated protein (MAP) cascade kinases responding to signal transduction, including MoMck1 (MAPKKK), MoMkk1 (MAPKK), and MoMps1 (MAPK) [22]. Diverse signal pathways identified have crosstalk with CWI, suggesting the central role of CWI in fungal growth and pathogenicity [23–26].

We previously found a gene encoding a hypothetical protein with a signal peptide and transmembrane domain by comparative genomics analysis, which might be involved in fungal virulence, but the functions of this gene were unknown. In this study, the gene-deletion mutants displayed compromised hypha growth, and the gene was named *MoHG1* (hypha growth gene in *M. oryzae*). *MoHG1* positively regulates fungal development and infection by maintaining CWI. Moreover, the decreased content of chitin was found in the  $\Delta$ *Mohg1* mutant. Combined with transcriptomic results, many genes in MAPK and sugar metabolism pathways are significantly regulated in the  $\Delta$ *Mohg1* mutant. A hexokinase gene, *MGG\_00623* was downregulated in  $\Delta$ *Mohg1* according to transcriptome results. We overexpressed *MGG\_00623* in a  $\Delta$ *Mohg1* mutant. The results showed that fungal growth and chitin contents in *MGG\_00623*-overexpressing strains were restored significantly compared to the  $\Delta$ *Mohg1* mutant. Furthermore, *MoHG1* could interact with *MGG\_00623* directly through yeast two-hybrid and BiFC. These results provide valuable references for the genes with similar structures in *M. oryzae*.

## 2. Materials and Methods

### 2.1. Phylogenetic Analyses

The homolog sequences of *MoHG1* were downloaded from different rice- or non-rice-infecting isolates in the NCBI database. FastTree software (Version 2.1.10) was used for phylogenetic analysis. The phylogenetic tree plot was generated using ChiPlot (<https://www.chiplot.online>, accessed on 16 August 2024).

### 2.2. Culture Conditions

Wild-type *M. oryzae* YN125 and mutant strains conserved at Yunnan Agricultural University were cultured on a potato sucrose agar (PSA) medium for growth. Complete medium (CM) and minimum medium (MM) were used for growth assays with different stressor treatments. Oatmeal medium (OM) was used for sporulation. For quantitative analyses of spore production, germ tube, and appressorium formations, the conidia were harvested from OM and then filtered through two layers of Miracloth (Calbiochem, San

Diego, CA, USA). The spore suspensions were resuspended twice in sterile water. Spore production in a given colony was counted using a hemocytometer. The spore suspension was dropped on a microscope cover glass (Fisher Scientific, 12545100, Waltham, MA, USA), and the rates of germ tube and appressorium formations were recorded using a microscope. The experiments were performed in three biological repeats.

### 2.3. Infection Assays

The susceptible rice variety Lijiangxintuanheigu (LTH) was used for fungal inoculation. A spore suspension ( $1 \times 10^5$  spores/mL) was foliar-sprayed on 21-day-old rice seedlings. The inoculated seedlings were incubated in the dark for 24 h at 28 °C and transferred to the greenhouse for 6 days. At 7 days post-inoculation, the disease index was assessed. Fifteen seedlings were used for inoculation of each isolate, and there were three independent inoculation experiments. A disease score of 0–5 was assigned according to the lesion type. The disease index was calculated using the following formula.

$$\text{Disease index} = \frac{\sum(\text{disease score} \times \text{number of diseased leaves})}{\text{Total number of investigate leaves} \times 5} \times 100$$

### 2.4. Protoplast Release Assay

The fungi were grown in liquid yeast extraction and glucose media (YEG) for 2 days and then harvested. The dried mycelia were transferred into a lysis enzyme solution for 1 h. The released protoplast solution was dropped on a hemocytometer and the number of protoplasts was counted using a microscope [23–26].

### 2.5. Vector Construction and Transformation

The vector pCX62 was used for *MoHG1* gene deletion, and the 1000–2000 bp sequences upstream and downstream of the *MoHG1*-coding sequences were inserted into two flanking regions of the maker gene (hygromycin phosphotransferase, HPT), respectively. The constructed deletion vector was transformed into protoplasts of YN125 using the PEG–CaCl<sub>2</sub>-mediated method. The positive deleted transformants were confirmed using PCR with specific primers (Table S1). The native promoter and coding sequences of *MoHG1* were inserted into a pYF11 vector carrying a green fluorescent gene and transformed into YN125 for *MoHG1*-GFP observation. For *MGG\_00623*-overexpressing strain construction, coding sequences of *MGG\_00623* were inserted into pYF11 with the continuous expressing promoter *RP27* and transformed into a  $\Delta\text{Mohg1}$  mutant. The overexpression of *MGG\_00623* was confirmed via qRT-PCR.

### 2.6. Carbohydrate Content Assay

Fungal strains were grown in liquid YEG for 2 days. The mycelia of WT and  $\Delta\text{Mohg1}$  were dried using vacuum freezing and then ground into powder, respectively. 30 mg of the powder from each sample was diluted into a 500 µL solution containing methanol/isopropanol/water (3:3:2 v/v/v), vortexed for 3 min, and subjected to ultrasound for 30 min. The extraction was centrifuged at 4 °C and 14,000 r/min for 3 min. 20 µL suspensions were transferred to a new tube and added to 20 µL ribitol (100 µg/mL) as the internal standard. For the derivatization treatment, the mixture was dried using nitrogen gas and added to a 100 µL solution of methoxyamine hydrochloride in pyridine (15 mg/mL) for incubation at 37 °C for 2 h. Then, 100 µL of BSTFA was added to the mixture and maintained at 37 °C for 30 min.

An Agilent 7890 (Santa Clara, CA, USA) gas chromatograph coupled with a 5975C mass spectrometer with a DB-5MS column (30 m length  $\times$  0.25 mm i.d.  $\times$  0.25 µm film thickness, J&W Scientific, Folsom, CA, USA) was used for sugar detection. Helium was used as the carrier gas at a flow rate of 1 mL/min. Injections were performed in the splitless mode, and the injected volume was 2 µL. The oven temperature was maintained at 70 °C for 1 min, raised to 112 °C at 30 °C/min and maintained for 3 min, raised to 175 °C at

15 °C/min and maintained for 1 min, raised to 190 °C at 3 °C/min and maintained for 2 min, then raised to 240 °C at 35 °C/min, and finally raised to 280 °C at 10 °C/min and maintained at this temperature for 2.5 min. All samples were analyzed in the selective ion-monitoring mode. The ion source and transfer line temperatures were 230 °C and 240 °C, respectively.

The standard curve for each sugar was generated using the different concentrations of standard sugar solutions and corresponding mass spectrometer peak data. The sugar content was calculated using the following equation:  $\text{content (mg/g)} = c \times V1 \times V2 \div V3 \div m \div 1000000$  ( $c$  is the concentration generated by the standard curve according to the peak area of each sample;  $V1$  is the constant volume;  $V2$  is the extraction volume;  $V3$  is the collected suspension volume;  $m$  is the sample weight).

## 2.7. RNA Isolation and Quantitative Real-Time (qRT)-PCR

The RNA isolations from fungi and rice leaves were performed using the UNIQ-10 Column TRIzol Total RNA Isolation Kit (Sangon Biotech, B511321, Shanghai, China). PrimeScript IV 1st strand cDNA Synthesis Mix (Takara, 6215A, Shiga, Japan) was used for cDNA synthesis. The primers used for qRT-PCR are listed in Table S1. The *M. oryzae* actin gene *MGG\_03982* and the rice actin gene were used as the endogenous controls for normalization, respectively. The relative expressions of target genes were calculated using the  $2^{-\Delta\Delta C_t}$  method.

## 2.8. RNA Sequencing

The RNA sequencing methods for WT and  $\Delta\text{Mohg1}$  isolates were performed based on the previous protocols [27]. Fungal strains were grown in liquid YEG for 2 days and then the mycelia were collected for RNA isolation. Sequencing libraries were constructed using the Illumina Truseq™ RNA sample prep kit (San Diego, CA, USA) and sequenced on the Illumina Novaseq 6000 platform (San Diego, CA, USA). The raw data were uploaded to NCBI SRA under the BioProject number PRJNA1076595. Clean data were assembled using Cufflinks (Version 2.2.1) based on the reads mapped to the *M. oryzae* reference genome ([https://www.ncbi.nlm.nih.gov/assembly/GCF\\_000002495.2](https://www.ncbi.nlm.nih.gov/assembly/GCF_000002495.2), accessed on 16 August 2024), while unmapped reads were annotated with sequence alignment. The read count of each gene was generated by RSEM software (Version 1.3.3), DESeq2 (Version 1.10.1) was used to identify differentially expressed genes (DEGs), and the DEGs were filtered by  $|\log_2\text{FC}| \geq 1$ , with a Padjust value of <0.05. The GO and KEGG analyses were based on DAVID (<https://david.ncifcrf.gov/home.jsp>, accessed on 16 August 2024).

## 2.9. Cell Wall Staining and Chitin Content Assays

Calcofluor white (CFW) was used for fungal cell wall staining according to the methodology in a previous paper with a slight modification [23–26]. WT and  $\Delta\text{Mohg1}$  were grown in liquid YEG for 4 days and washed using ddH<sub>2</sub>O. The dried mycelia were soaked in 10 µg/mL CFW solution for 5 min and rinsed with ddH<sub>2</sub>O to wash off the dye. The cell wall staining was observed using a fluorescence microscope.

The chitin content assays for WT and  $\Delta\text{Mohg1}$  were conducted according to a previously published method [28]. WT and  $\Delta\text{Mohg1}$  were grown in liquid YEG for 4 days and washed using ddH<sub>2</sub>O. The chitin content was determined by measuring the amount of glucosamine released after the hydrolysis of the cell walls.

## 2.10. Yeast Two-Hybrid and BiFC Assays

For yeast two-hybrid, the CDS fragment of *MoHG1* was inserted into prey plasmid pPR3-N, while the CDS fragment of the *MGG\_00623* was cloned into bait plasmid pBT3-STE. The constructed vectors were co-transformed into competent cells of yeast NMY51 and incubated on a synthetic medium lacking leucine and tryptophan (SD–Leu–Trp) then were further transferred to a synthetic medium lacking leucine, tryptophan, adenine, and histidine (SD–Leu–Trp–Ade–His). For BiFC observation, the CDS regions of *MGG\_00623*



and *MoHG1* were cloned into pSm35s-nYFP and pSm35s-cYFP vectors, respectively. The pSm35s::nYFP::MGG\_00623 and pSm35s::MoHG1::cYFP were co-inoculated into tobacco leaves through agrobacterium-mediated transformation and incubated for 2 days. The YFP was observed under a laser scanning confocal microscope.

### 3. Results

#### 3.1. *MoHG1* Influence the Fungal Development

*MoHG1* encodes 201 amino acids with a 24-amino acid signal peptide and possesses 3 transmembrane domains. There is one nonsynonymous substitution at the 106th amino acid locus between *MoHG1* and MGG\_14388 in the 70–15 reference strain genome (Figure 1A). We aligned the sequences of *MoHG1* in the genomes of rice and non-rice lineage isolates and found that the sequences in rice lineage were generally clustered together while the sequences in non-rice lineages belonged to another subgroup (Figure 1B).

Two  $\Delta$ *Mohg1* mutants were screened using PCR (Figure S1), and the hyphal growth of both  $\Delta$ *Mohg1* mutants was compromised when they were grown on the CM and MM plates compared with the wild type. Moreover, spore production, germination, and appressorium formation were also decreased in the  $\Delta$ *Mohg1* mutants (Figure 1C–H). These results indicate that *MoHG1* affects fungal development.

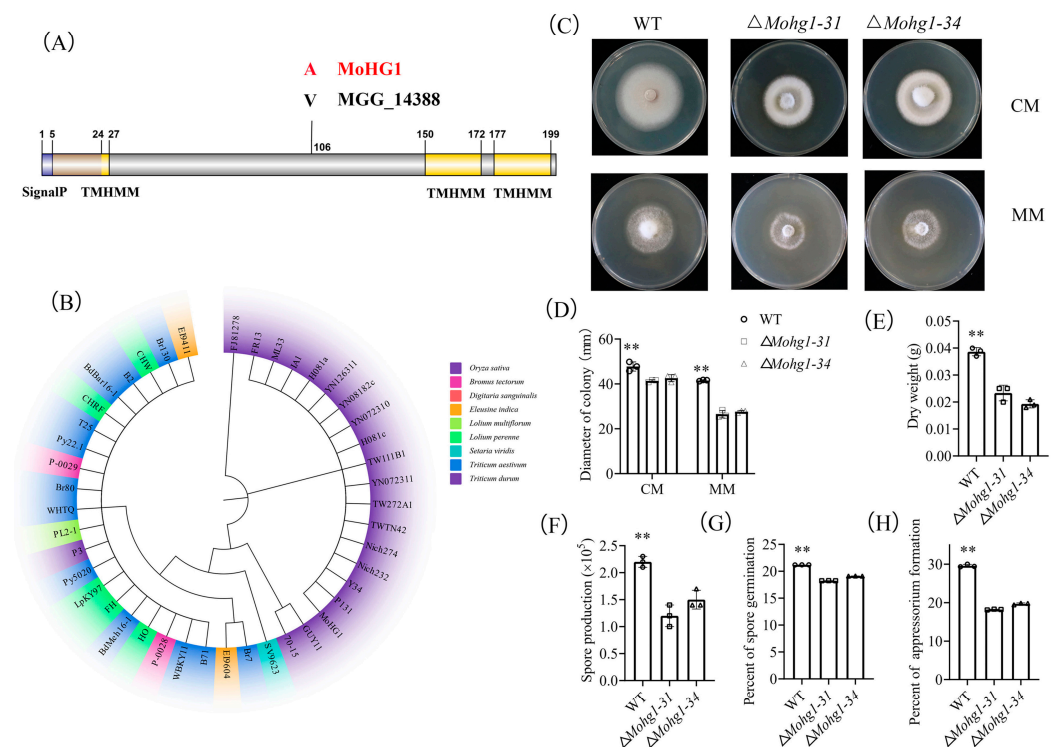


**Figure 1.** *MoHG1* influences the fungal development. (A) The amino acid sequence alignment between *MoHG1* and MGG\_14388. (B) Phylogenetic analyses of *MoHG1* homologous sequences in different host-infecting strains. (C) Colonic phenotypes of  $\Delta$ *Mohg1* at CM and MM plates. (D–H) The diameter of the colony, dry weight, spore production, spore germination, and appressorium formation. Each experiment was conducted with 3 biological repeats and statistically significant differences were calculated by Student's *t*-test, \*\*  $p < 0.01$ . Error bars represent the means  $\pm$  SD.

#### 3.2. *MoHG1* Regulates Fungal Cell Wall Integrity in *M. oryzae*

Congo red (CR), sodium dodecyl sulfate (SDS), and calcofluor white (CFW) are often used to assess fungal cell wall integrity. *Mohg1* mutants were more sensitive to CR, SDS, and CFW than WT (Figure 2A,B). Similarly, osmotic stressors such as sorbitol, KCl, and NaCl show stronger inhibition in  $\Delta$ *Mohg1* mutants (Figure 2C,D). Moreover, fungal mycelia were treated with cell wall-degrading enzymes. The results showed more protoplasts

were released by  $\Delta MoHg1$  mutants than WT at 1 h post-treatment (Figure 2E,F). The fungal cell wall of each strain was stained by CFW, and there was a stronger fluorescence signal observed in WT than in the  $\Delta MoHg1$  (Figure 2G). These results indicate that fungal cell wall integrity was disrupted in  $\Delta MoHg1$  mutants, and MoHG1 plays an important role in maintaining CWI.

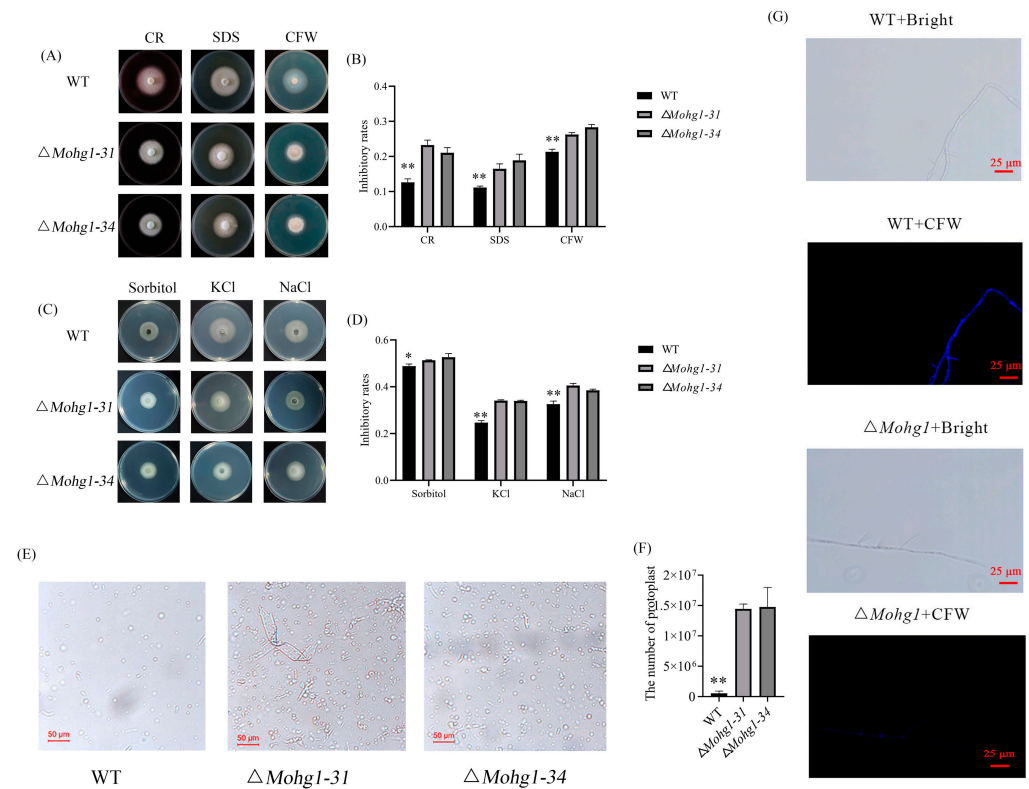


**Figure 2.** *MoHG1* regulates fungal cell wall integrity in *M. oryzae*. (A,B)  $\Delta MoHg1$  mutants show more sensitivity to CR (600  $\mu\text{g}/\text{mL}$ ), SDS (100  $\mu\text{g}/\text{mL}$ ), and CFW (4  $\mu\text{g}/\text{mL}$ ). (C,D)  $\Delta MoHg1$  mutants show more sensitivity to sorbitol (1 mol/L), KCl (0.7 mol/L), and NaCl (0.7 mol/L). (E,F) The released protoplast in WT and  $\Delta MoHg1$  mutants. Each experiment was conducted with 3 biological repeats and statistically significant differences were calculated by Student's *t*-test, \*  $p < 0.05$ , \*\*  $p < 0.01$ . Error bars represent the means  $\pm$  SD. (G) The fungal cell wall staining in  $\Delta MoHg1$  and WT.

### 3.3. *MoHG1* Plays an Essential Role in Pathogenicity

To investigate the role of *MoHG1* in pathogenesis, spore suspensions of WT and  $\Delta MoHg1$  mutants were sprayed onto rice seedlings. At day 7 post-inoculation, typically infectious lesions were formed by WT, while a smaller number of lesions were caused by the  $\Delta MoHg1$  mutants (Figure 3A). Pathogenicity assay showed that the disease index of WT was much higher than that of the mutants (Figure 3B). Moreover, some basal defense genes such as *OsMPK5*, *OsMPK6*, *OsMPK12*, *OsPAD4*, and *OsEDS1* were upregulated in the rice inoculated with  $\Delta MoHg1-31$  (Figure 3C–G). The fragments containing *MoHG1*-GFP with its native promoter were transferred into an mCherry fluorescent protein tagged strain YN125. The fluorescent signal of *MoHG1*-GFP was observed in spore and infectious mycelia during infection (Figure 3H). These results suggest that the expressions of *MoHG1* can be induced and affect fungal pathogenicity during infection.

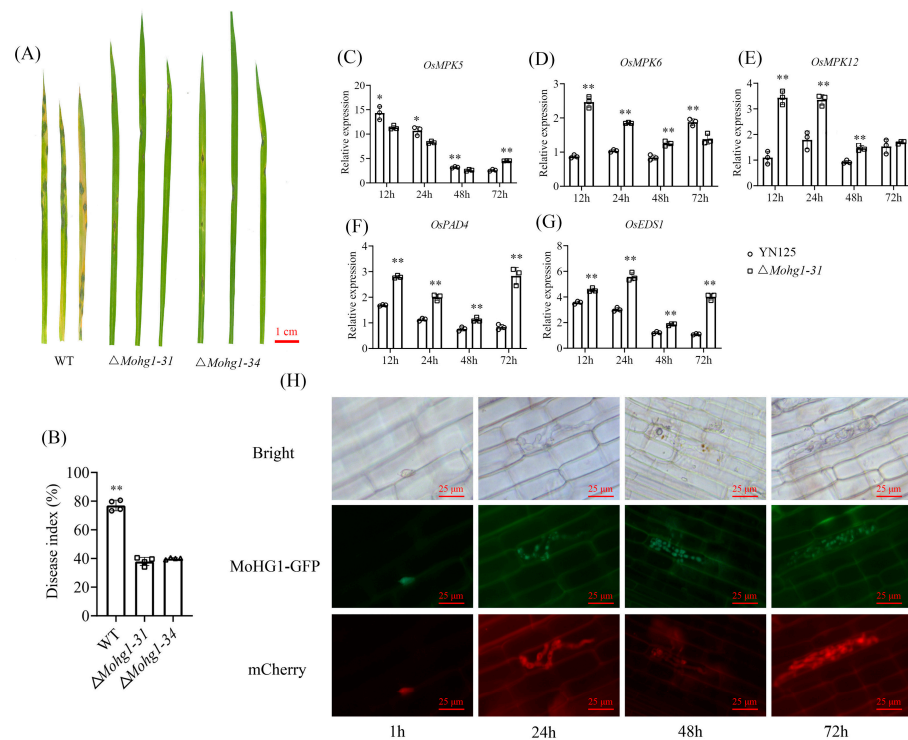


**Figure 3.** *MoHG1* plays an essential role in pathogenicity. (A,B) The pathogenicity of  $\Delta MoHG1$  mutants on rice. (C–G) The expressions of basal defense genes in rice inoculated by  $\Delta MoHG1$  and WT. (H) The fluorescent signal of MoHG1-GFP in *M. oryzae* during infection. Each experiment was conducted with 3 biological repeats and statistically significant differences were calculated by Student's *t*-test, \*  $p < 0.05$ , \*\*  $p < 0.01$ . Error bars represent the means  $\pm$  SD.

### 3.4. Sugar and MAPK Pathways Are Regulated in $\Delta MoHG1$ by Transcriptome Analysis

Transcriptomic analysis was performed to explore the expression patterns characterized by *MoHG1*. There were 2394 upregulated genes and 1581 downregulated genes in the  $\Delta MoHG1$  mutant compared with WT (Figure 4A). Based on the GO and KEGG results, the downregulated genes were mainly enriched in RNA transcription, an integral component of the membrane, nucleolus, MAPK signaling pathway, and cell cycle (Figure 4B). Meanwhile, the upregulated genes were related to translation, methylation, the carbohydrate metabolic process, ribosome, pentose, and glucuronate interconversion-related biological processes in the  $\Delta MoHG1$  mutant (Figure 4C). Based on the pentose and glucuronate interconversion pathway, there were many upregulated genes involved in the glycerol and xylitol metabolism (Figure 4D,E). Moreover, there were many downregulated genes in the MAPK pathway in the  $\Delta MoHG1$  mutant (Figure 4F). Thus, transcriptome analysis indicated that *MoHG1* could regulate sugar and MAPK pathways to affect fungal growth.

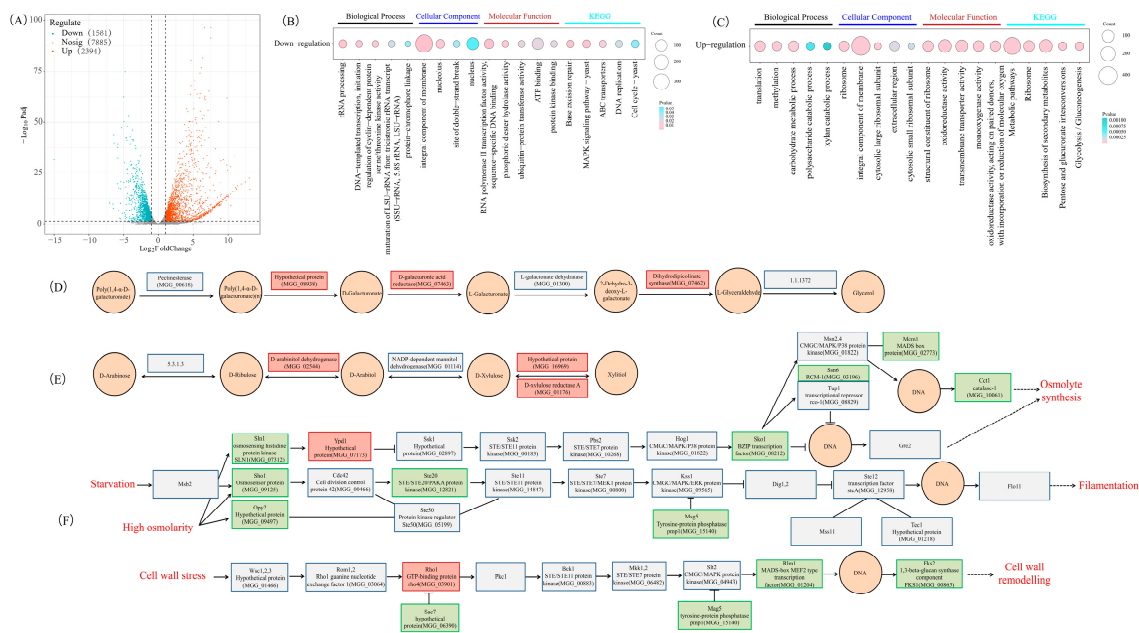


**Figure 4.** Transcriptome analysis between WT and  $\Delta Mohg1$ . (A) The volcano plot of DEGs in  $\Delta Mohg1$ . GO enrichment and KEGG pathway analysis of downregulated (B) and upregulated (C) genes in  $\Delta Mohg1$ . The DEGs involving glycerol synthesis (D), synthesis pentose (E), and MAPK pathway (F) in *M. oryzae*. The box background in green or red means the decrease or increase of gene expression according to the transcriptome, respectively.

### 3.5. MoHG1 Influences the Contents of Some Carbohydrates

According to the KEGG analyses, we found carbohydrate metabolism-related genes were upregulated in the  $\Delta Mohg1$  mutant. Thus, the contents of carbohydrates, including arabinose, fructose, sorbitol, glucose, inositol, lactose, rhamnose, and xylitol were measured. The results showed that the contents of arabinose, sorbitol, lactose, rhamnose, and xylitol were significantly higher in the  $\Delta Mohg1$  mutant than in WT (Figure 5A–H). The results show that *MoHG1* influences the contents of some carbohydrates to regulate fungal growth in *M. oryzae*.

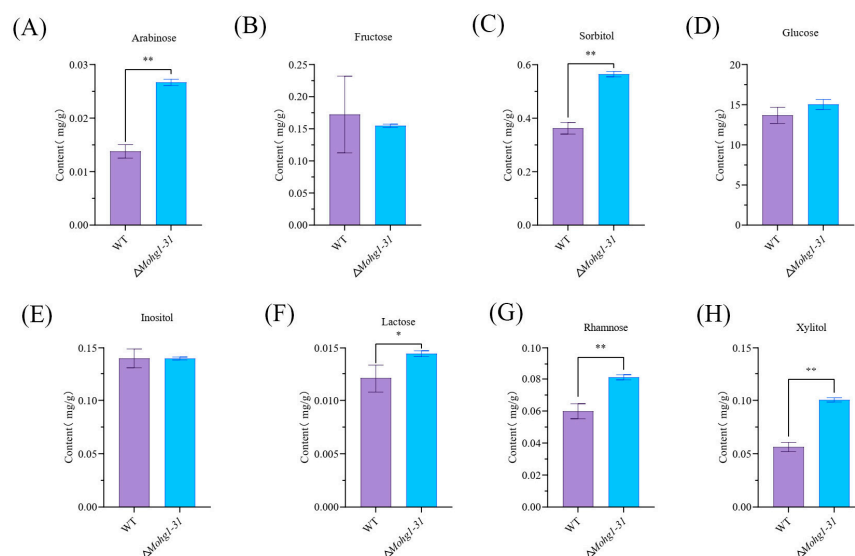


**Figure 5.** The carbohydrate contents in  $\Delta Mohg1$ . (A–H) The content of 8 carbohydrates. Each experiment was conducted with 3 biological repeats and statistically significant differences were calculated by Student's *t*-test, \*  $p < 0.05$ , \*\*  $p < 0.01$ . Error bars represent the means  $\pm$  SD.

### 3.6. Overexpressing of *MGG\_00623* in $\Delta$ *Mohg1* Mutant Restored the Fungal Growth and Chitin Contents

Transcriptomic analysis indicated that *MoHG1* could affect cell wall integrity and carbohydrate metabolism. Coincidentally, the contents of some carbohydrates and chitin were also disrupted in  $\Delta$ *Mohg1* compared with WT (Figures 2G and 5). For the downregulated genes in  $\Delta$ *Mohg1*, *MGG\_00623* encodes a hexokinase, which may be associated with carbohydrates and chitin metabolism. Thus, *MGG\_00623* was overexpressed in  $\Delta$ *Mohg1* mutants and two overexpression strains were obtained (Figure 6A). We found that the colony diameters of overexpressing strains were greater than  $\Delta$ *Mohg1* (Figure 6B,C). Moreover, the CFW staining and chitin contents were restored significantly in overexpressing strains, suggesting the overexpressing of *MGG\_00623* could promote the CWI (Figure 6D,E). We also found that *MoHG1* could interact with *MGG\_00623* directly through yeast two-hybrid and BiFC (Figure 6F,G). Thus, our results showed that *MoHG1* could interact with *MGG\_00623* and the overexpressing of *MGG\_00623* in the  $\Delta$ *Mohg1* mutant could restore the fungal growth and chitin contents.

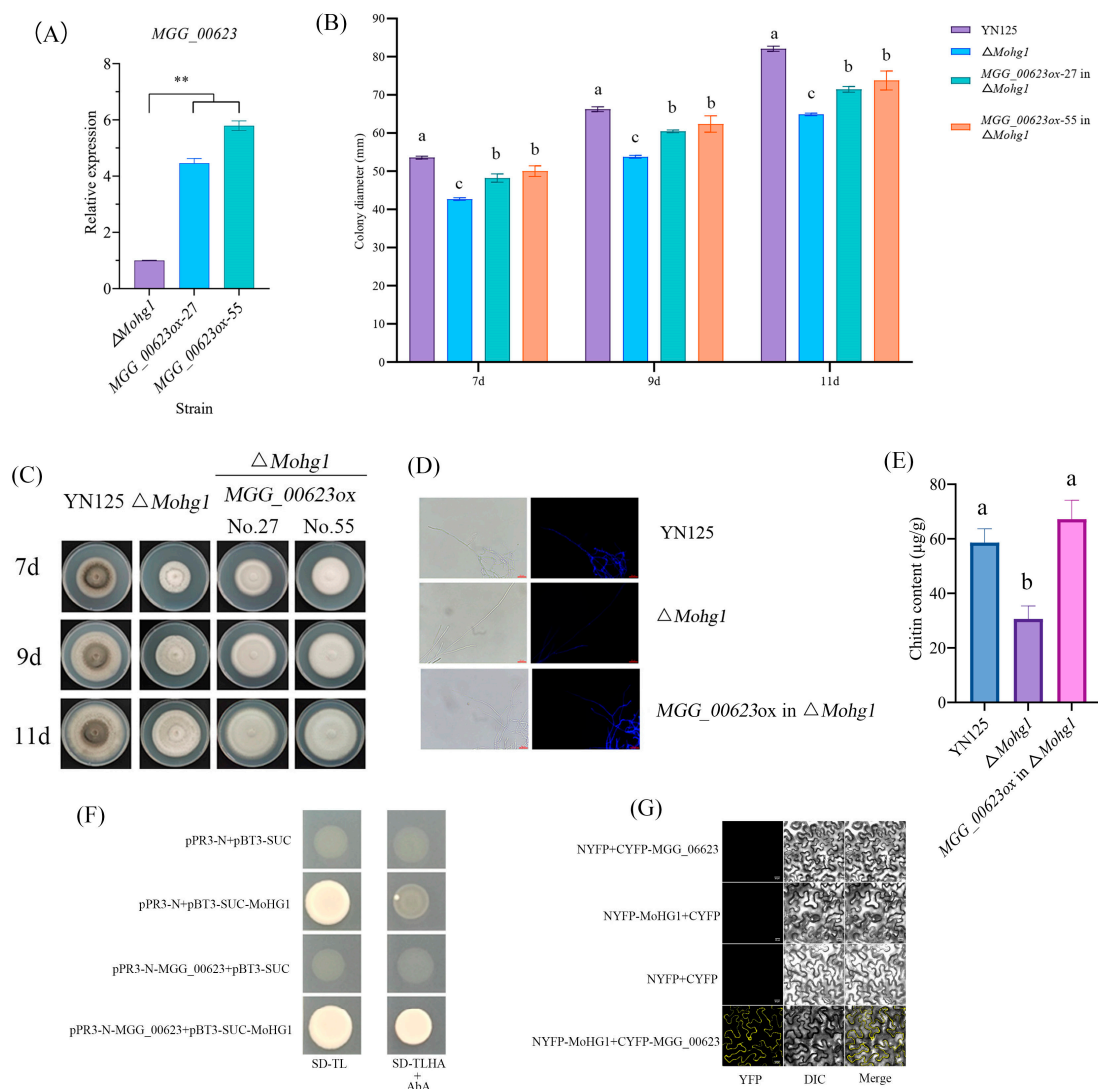


**Figure 6.** Overexpressing of *MGG\_00623* in the  $\Delta$ *Mohg1* mutant restored the fungal growth and chitin contents. (A) The relative expressions of *MGG\_00623* in  $\Delta$ *Mohg1*. Each experiment was conducted



with 3 biological repeats and statistically significant differences were calculated by Student's *t*-test, \*\*  $p < 0.01$ . (B,C) Overexpression of *MGG\_00623* in  $\Delta$ *Mohg1* partially restored the fungal growth. Each experiment was conducted in 3 biological repeats. The different letters above each bar graph indicate significant differences ( $p < 0.05$ ) calculated by ANOVA and Duncan's test. Error bars represent the means  $\pm$  SD. (D,E) Overexpression of *MGG\_00623* in  $\Delta$ *Mohg1* restored CWI staining and chitin contents. The scale bar represents 25  $\mu$ m. The different letters above each bar graph indicate significant differences ( $p < 0.05$ ) calculated by ANOVA and Duncan's test. Error bars represent the means  $\pm$  SD. (F) Yeast two-hybrid and (G) BiFC assays show MoHG1 interacts with *MGG\_00623*. The scale bar represents 20  $\mu$ m.

## 4. Discussion

### 4.1. MoHG1 Is Required for Development and Pathogenicity of *M. oryzae*

In this study, we have identified a gene, *MoHG1*, involved in fungal development and pathogenicity in *M. oryzae*. *MoHG1* in the *M. oryzae* Oryza pathotype is more conserved than in other pathotypes, indicating that this gene might be associated with the differentiation of the Oryza pathotype in *M. oryzae* populations (Figure 1B). *MoHG1* possesses typical signal peptide and transmembrane domains, but the protein could not be secreted into the extracellular space and cytoplasm in rice under microscope observation (Figures 1A and 3H). Moreover, previous secretome results did not identify this protein during the infection of *M. oryzae* [29]. A similar structural protein, PRO41, harboring a signal sequence and three transmembrane domains, was identified in *Sordaria macrospora*, which is located in the endoplasmic reticulum (ER) membrane and is essential for sexual development [30]. These results suggested that *MoHG1* affected pathogenicity by regulating fungal development, not by being secreted into rice cells to disrupt host defense.

$\Delta$ *Mohg1* mutants display compromised fungal development and pathogenicity compared with the wild type (Figures 1C–H and 3A). These results suggest that *MoHG1* plays an important role in fungal development and infection. Based on transcriptome analysis (Table S2), many transcription factor (TF) genes were downregulated in the  $\Delta$ *Mohg1* mutant. *Con7* regulates appressorium formation [31]. Homeobox TF family genes, such as *MoHOX2* and *MoHOX4*, are essential for conidiogenesis [32]. *Com1*, *Moatf1*, and *MoMcm1* are required for fungal development and virulence [33–35]. Thus, *MoHG1* might affect the expression of some TF genes to regulate downstream genes to influence development and pathogenicity in *M. oryzae*.

Many innate immune-related genes were upregulated in rice inoculated with the  $\Delta$ *Mohg1* mutant (Figure 3C). The MAPK cascade genes *OsMPK6* and *OsMPK12* (*OsBWMK1*) were upregulated, which were associated with the *WRKY45*- and *OsWRKY33*-mediated SA signaling pathways, respectively [36]. Furthermore, *OsPAD4* and *OsEDS1* involved in the SA pathway were also induced by the  $\Delta$ *Mohg1* mutant. These results suggested that the activation of an SA pathway in rice enhances the resistance with  $\Delta$ *Mohg1*. Effectors secreted by pathogens that interfere with the SA pathway have been identified. In *M. oryzae*, two nuclear effector gene deletion mutants,  $\Delta$ *Mohtr1* and  $\Delta$ *Mohtr2*, also induce expressions of SA-related genes when they were inoculated [37]. Interestingly, many genes encoding cell death-inducing proteins (CDIPs) [38,39] were upregulated in the  $\Delta$ *Mohg1* mutant (Table S2) and cell death is regarded as an immunity response to pathogens. However, whether a  $\Delta$ *Mohg1* mutant could secrete more cell death-inducing proteins into rice cells and trigger SA-mediated immunity needs further research.

### 4.2. MoHG1 Regulates Signal Sensors and Cell Wall Integrity in *M. oryzae*

In *M. oryzae*, signal transduction from the cell surface into the cell through a series of phosphorylation cascades, such as the cyclic AMP-dependent protein kinase A (cAMP/PKA) signaling pathway [40], the Pmk1 MAPK pathway [41,42], and the CWI pathway, have been well identified [22,43]. The crosstalk among these pathways can coordinate them with each other to regulate fungal behavior. According to the KEGG results, many downregulated genes were enriched in the MAPK signaling pathway (Figure 4B). We

found that the expressions of four sensor genes, *MoSho1*, *MoOpy2*, *Sln1*, and *PTH11* were downregulated in the  $\Delta$ *Mohg1* mutant (Table S2). *MoSho1* functions by recognizing rice leaf waxes for Pmk1 activation and appressorium formation [21]. *MoOpy2* participates in the *Osm1* MAPK pathway and the *Mps1* MAPK pathway to regulate fungal development, pathogenicity, and autophagy [44]. *Sln1* is responsible for sensing the turgor threshold to affect penetration into rice leaves [45]. *PTH11* as a G-protein-coupled receptor influences the MAPK Pmk1 and cAMP/PKA pathways to regulate appressorium [18]. In summary, *MoHG1* influences the expressions of sensor genes to regulate signal transduction.

The  $\Delta$ *Mohg1* mutants showed more sensitivity to CWI stressors and more easily released protoplasts under lysis enzyme treatment (Figure 2). The CWI pathway is essential to pathogen development and infection. The core components of the CWI pathway have been well identified, but *MoMck1*, *MoMkk1*, and *MoMps1* were not significantly regulated in the  $\Delta$ *Mohg1* mutant. However, *MoSLN1*, *MoGln2*, and *Gel5* were reported to participate in CWI [13,46,47] and downregulated in the  $\Delta$ *Mohg1* mutant. Thus, *MoHG1* may affect the expressions of CWI-related genes to maintain fungal cell wall integrity.

#### 4.3. *MoHG1* Interacts with a Hexokinase to Mediate Carbohydrate and Chitin Metabolism

Pentose and glucuronate interconversion pathway and glycolysis/gluconeogenesis pathway-related genes were significantly enriched in the  $\Delta$ *Mohg1* mutant (Figure 4C), and the contents of arabinose, sorbitol, lactose, rhamnose, and xylitol were also higher in  $\Delta$ *Mohg1* (Figure 5A,C,F–H). Interestingly, we also found many genes involving lactose, arabinol, and xylitol metabolism upregulated in the  $\Delta$ *Mohg1* mutant (Figure 4C–E). The glycolysis/gluconeogenesis pathway is responsible for the breakdown of glucose into pyruvate, which can be further converted into lactate by L-lactate dehydrogenase [48]. The  $\Delta$ *Mohg1* mutant was cultured in a nutrition-rich medium, which could provide sufficient glucose for growth, and thus the content of glucose in the  $\Delta$ *Mohg1* mutant is similar to that in WT. Arabinose and xylitol are the metabolites of the pentose catabolic pathway [49]. The expressions of the D-arabinol dehydrogenase and D-xylulose reductase A were upregulated in the  $\Delta$ *Mohg1* mutant, and were consistent with higher contents of arabinose and xylitol in  $\Delta$ *Mohg1*. These results suggest that *MoHG1* negatively regulates some aspects of carbohydrate metabolism. However, the relationship between higher contents and growth defect regulated by *MoHG1* in *M. oryzae* needs further research.

Fungal chitin is required for growth and virulence in *M. oryzae*. We found that the cell wall integrity was disrupted, and the content of chitin was also decreased in  $\Delta$ *Mohg1*. There are seven chitin synthase (CHS) genes identified in *M. oryzae* [50]. Based on transcriptome analysis, *CHS1* and *CHS3* were downregulated, while *CHS2* and *CHS7* were upregulated in  $\Delta$ *Mohg1*, which could affect chitin content (Table S2). Based on transcriptome results, many genes were downregulated that were involved in carbohydrate and chitin metabolism. These results might indicate that *MoHG1* could be an upstream component to regulate fungal carbohydrate and chitin metabolism. For the downregulated genes, *MGG\_00623* encodes a hexokinase-1, which is regarded as the first enzyme to catalyze the conversion of glucose into glucose-6-phosphate in the glycolysis pathway, while glucose-6-phosphate can be converted into fructose-6-phosphate as the primary material for chitin synthesis in the hexosamine pathway. Many studies have shown that hexokinase-mediated glucose utilization can positively affect chitin synthesis in insects [51–53]. Our results indicate that *MGG\_00623* could play a more important role in *MoHG1* mediating fungal growth and virulence via the sugar and chitin metabolism pathway. Moreover, *MGG\_00623* could interact with *MoHG1* directly, which might remodel the *MGG\_00623* structure and enhance the hexokinase activity to increase the chitin production in *M. oryzae*. However, our results demonstrate that *MoHG1* affects fungal growth and virulence through regulating CWI and chitin content. The molecular mechanisms of interactions among *MoHG1*, CWI, and chitin synthesis-related proteins still require further research.

**Supplementary Materials:** The following supporting information can be downloaded at: <https://www.mdpi.com/article/10.3390/jof10090663/s1>, Figure S1: The confirmation of  $\Delta Mohg1$  mutants by PCR; Table S1: The primers used in this study; Table S2: The DEGs in  $\Delta Mohg1$  compared with WT.

**Author Contributions:** Conceptualization, Y.W. and C.L.; methodology, X.P. and A.L.; validation S.M.J.; formal analysis, C.W.; investigation, X.Y. and K.Y.; resources, X.P.; writing—original draft preparation, Y.W.; writing—review and editing, C.L.; funding acquisition, Y.W. and C.L. All authors have read and agreed to the published version of the manuscript.

**Funding:** This work was supported by the National Key R&D Program of China (2023YFD1400800), the National Natural Science Foundation of China (32202254), Major Science and Technology Projects in Yunnan (202402AE090026), the Yunnan Provincial Talent Program for Wang Yi (XDYC-QNRC-2023-0421), Basic Research Special Project in Yunnan (202201AT070255, 202401BD070001-013).

**Institutional Review Board Statement:** Not applicable.

**Informed Consent Statement:** Not applicable.

**Data Availability Statement:** The raw data were uploaded to NCBI SRA under the BioProject number PRJNA1076595. [SUB14224803] [<https://submit.ncbi.nlm.nih.gov/subs/sra/SUB14224803/overview>], accessed on 16 August 2024 [SUB14224803].

**Conflicts of Interest:** The authors declare no conflicts of interest.

## References

1. Fernandez, J.; Orth, K. Rise of a Cereal Killer: The Biology of *Magnaporthe oryzae* Biotrophic Growth. *Trends Microbiol.* **2018**, *26*, 582–597. [[CrossRef](#)] [[PubMed](#)]
2. Yan, X.; Talbot, N.J. Investigating the cell biology of plant infection by the rice blast fungus *Magnaporthe oryzae*. *Curr. Opin. Microbiol.* **2016**, *34*, 147–153. [[CrossRef](#)] [[PubMed](#)]
3. Gladieux, P.; Condon, B.; Ravel, S.; Soanes, D.; Maciel, J.L.N.; Nhani, A., Jr.; Chen, L.; Terauchi, R.; Lebrun, M.-H.; Tharreau, D.J. Gene flow between divergent cereal- and grass-specific lineages of the rice blast fungus *Magnaporthe oryzae*. *Mbio* **2018**, *9*, 10–1128. [[CrossRef](#)] [[PubMed](#)]
4. Rahnama, M.; Condon, B.; Ascari, J.P.; Dupuis, J.R.; Del Ponte, E.M.; Pedley, K.F.; Martinez, S.; Valent, B.; Farman, M.L. Recent co-evolution of two pandemic plant diseases in a multi-hybrid swarm. *Nat. Ecol. Evol.* **2023**, *7*, 2055–2066. [[CrossRef](#)] [[PubMed](#)]
5. Wu, Q.; Wang, Y.; Liu, L.-N.; Shi, K.; Li, C.-Y.J. Comparative genomics and gene pool analysis reveal the decrease of genome diversity and gene number in rice blast fungi by stable adaption with rice. *J. Fungi* **2021**, *8*, 5. [[CrossRef](#)]
6. Gow, N.A.R.; Latge, J.-P.; Munro, C.A.; Heitman, J. The Fungal Cell Wall: Structure, Biosynthesis, and Function. *Microbiology Spectrum* **2017**, *5*, 3. [[CrossRef](#)]
7. Geoghegan, I.; Steinberg, G.; Gurr, S. The Role of the Fungal Cell Wall in the Infection of Plants. *Trends Microbiol.* **2017**, *25*, 957–967. [[CrossRef](#)]
8. Lenardon, M.D.; Munro, C.A.; Gow, N.A.R. Chitin synthesis and fungal pathogenesis. *Curr. Opin. Microbiol.* **2010**, *13*, 416–423. [[CrossRef](#)]
9. Yang, C.; Yu, Y.; Huang, J.; Meng, F.; Pang, J.; Zhao, Q.; Islam, M.A.; Xu, N.; Tian, Y.; Liu, J. Binding of the *Magnaporthe oryzae* chitinase MoChia1 by a rice tetratricopeptide repeat protein allows free chitin to trigger immune responses. *Plant Cell* **2019**, *31*, 172–188. [[CrossRef](#)]
10. Mentlak, T.A.; Kombrink, A.; Shinya, T.; Ryder, L.S.; Otomo, I.; Saitoh, H.; Terauchi, R.; Nishizawa, Y.; Shibuya, N.; Thomma, B.P. Effector-mediated suppression of chitin-triggered immunity by *Magnaporthe oryzae* is necessary for rice blast disease. *Plant Cell* **2012**, *24*, 322–335. [[CrossRef](#)]
11. Zhu, S.; Yan, Y.; Qu, Y.; Wang, J.; Feng, X.; Liu, X.; Lin, F.; Lu, J. Role refinement of melanin synthesis genes by gene knockout reveals their functional diversity in *Pyricularia oryzae* strains. *Microbiol. Res.* **2021**, *242*, 126620. [[CrossRef](#)] [[PubMed](#)]
12. Collemare, J.; Billard, A.; Böhnert, H.U.; Lebrun, M.-H. Biosynthesis of secondary metabolites in the rice blast fungus *Magnaporthe grisea*: The role of hybrid PKS-NRPS in pathogenicity. *Mycol. Res.* **2008**, *112*, 207–215. [[CrossRef](#)] [[PubMed](#)]
13. Samalova, M.; Mélida, H.; Vilaplana, F.; Bulone, V.; Soanes, D.M.; Talbot, N.J.; Gurr, S.J. The  $\beta$ -1,3-glucanosyltransferases (Gels) affect the structure of the rice blast fungal cell wall during appressorium-mediated plant infection. *Cell. Microbiol.* **2016**, *19*, e12659. [[CrossRef](#)] [[PubMed](#)]
14. Adnan, M.; Zheng, W.; Islam, W.; Arif, M.; Abubakar, Y.; Wang, Z.; Lu, G. Carbon Catabolite Repression in Filamentous Fungi. *Int. J. Mol. Sci.* **2017**, *19*, 48. [[CrossRef](#)] [[PubMed](#)]
15. Hynes, M.; Fernandez, J.; Wright, J.D.; Hartline, D.; Quispe, C.F.; Madayiputhiya, N.; Wilson, R.A. Principles of Carbon Catabolite Repression in the Rice Blast Fungus: Tps1, Nmr1-3, and a MATE-Family Pump Regulate Glucose Metabolism during Infection. *PLoS Genet.* **2012**, *8*, e1002673. [[CrossRef](#)]

16. Fernandez, J.; Wilson, R.A. The sugar sensor, trehalose-6-phosphate synthase (Tps1), regulates primary and secondary metabolism during infection by the rice blast fungus: Will *Magnaporthe oryzae*'s "sweet tooth" become its "Achilles' heel"? *Mycology* **2011**, *2*, 46–53. [\[CrossRef\]](#)
17. Hong, Y.; Cai, R.; Guo, J.; Zhong, Z.; Bao, J.; Wang, Z.; Chen, X.; Zhou, J.; Lu, G. Carbon catabolite repressor MoCreA is required for the asexual development and pathogenicity of the rice blast fungus. *Fungal Genet. Biol.* **2021**, *146*, 103496. [\[CrossRef\]](#)
18. Kou, Y.; Tan, Y.H.; Ramanujam, R.; Naqvi, N.I. Structure–function analyses of the Pth11 receptor reveal an important role for CFEM motif and redox regulation in rice blast. *New Phytol.* **2016**, *214*, 330–342. [\[CrossRef\]](#)
19. Soanes, D.M.; Kershaw, M.J.; Cooley, R.N.; Talbot, N.J.J. Regulation of the MPG1 hydrophobin gene in the rice blast fungus *Magnaporthe grisea*. *Mol. Plant-Microbe Interact.* **2002**, *15*, 1253–1267. [\[CrossRef\]](#)
20. Kim, S.; Ahn, I.P.; Rho, H.S.; Lee, Y.H.J.M.M. MHP1, a *Magnaporthe grisea* hydrophobin gene, is required for fungal development and plant colonization. *Mol. Plant-Microbe Interact.* **2005**, *57*, 1224–1237. [\[CrossRef\]](#)
21. Liu, W.; Zhou, X.; Li, G.; Li, L.; Kong, L.; Wang, C.; Zhang, H.; Xu, J. Multiple plant surface signals are sensed by different mechanisms in the rice blast fungus for appressorium formation. *PLoS Pathog.* **2011**, *7*, e1001261. [\[CrossRef\]](#) [\[PubMed\]](#)
22. Jeon, J.; Goh, J.; Yoo, S.; Chi, M.-H.; Choi, J.; Rho, H.-S.; Park, J.; Han, S.-S.; Kim, B.R.; Park, S.-Y. A putative MAP kinase kinase, MCK1, is required for cell wall integrity and pathogenicity of the rice blast fungus, *Magnaporthe oryzae*. *Mol. Plant-Microbe Interact.* **2008**, *21*, 525–534. [\[CrossRef\]](#) [\[PubMed\]](#)
23. Guo, H.-S.; Feng, W.; Yin, Z.; Wu, H.; Liu, P.; Liu, X.; Liu, M.; Yu, R.; Gao, C.; Zhang, H.; et al. Balancing of the mitotic exit network and cell wall integrity signaling governs the development and pathogenicity in *Magnaporthe oryzae*. *PLOS Pathog.* **2021**, *17*, e1009080. [\[CrossRef\]](#)
24. Cai, Y.; Liu, X.; Shen, L.; Wang, N.; He, Y.; Zhang, H.; Wang, P.; Zhang, Z. Homeostasis of cell wall integrity pathway phosphorylation is required for the growth and pathogenicity of *Magnaporthe oryzae*. *Mol. Plant Pathol.* **2022**, *23*, 1214–1225. [\[CrossRef\]](#)
25. Yin, Z.; Tang, W.; Wang, J.; Liu, X.; Yang, L.; Gao, C.; Zhang, J.; Zhang, H.; Zheng, X.; Wang, P.; et al. Phosphodiesterase MoPdeH targets MoMck1 of the conserved mitogen-activated protein (MAP) kinase signalling pathway to regulate cell wall integrity in rice blast fungus *Magnaporthe oryzae*. *Mol. Plant Pathol.* **2015**, *17*, 654–668. [\[CrossRef\]](#)
26. Yin, Z.; Feng, W.; Chen, C.; Xu, J.; Li, Y.; Yang, L.; Wang, J.; Liu, X.; Wang, W.; Gao, C.; et al. Shedding light on autophagy coordinating with cell wall integrity signaling to govern pathogenicity of *Magnaporthe oryzae*. *Autophagy* **2019**, *16*, 900–916. [\[CrossRef\]](#)
27. Wang, Y.; Pu, X.; Ma, C.; Wang, Z.; Wu, Q.; Yang, C.; Liu, L.; Li, Y.; Wei, M.; Shi, Y. Multiomics Analyses Reveal the Complexity of Interaction between Two Strains of *Magnaporthe oryzae*. *J. Agric. Food Chem.* **2023**, *71*, 9706–9717. [\[CrossRef\]](#)
28. Liu, Y.; Shen, S.; Hao, Z.; Wang, Q.; Zhang, Y.; Zhao, Y.; Tong, Y.; Zeng, F.; Dong, J. Protein kinase A participates in hyphal and appressorial development by targeting Efg1-mediated transcription of a Rab GTPase in *Setosphaeria turcica*. *Mol. Plant Pathol.* **2022**, *23*, 1608–1619. [\[CrossRef\]](#)
29. Kim, S.G.; Wang, Y.; Lee, K.H.; Park, Z.-Y.; Park, J.; Wu, J.; Kwon, S.J.; Lee, Y.-H.; Agrawal, G.K.; Rakwal, R.; et al. In-depth insight into in vivo apoplast secretome of rice-*Magnaporthe oryzae* interaction. *J. Proteom.* **2013**, *78*, 58–71. [\[CrossRef\]](#)
30. Nowrousian, M.; Frank, S.; Koers, S.; Strauch, P.; Weitner, T.; Ringelberg, C.; Dunlap, J.C.; Loros, J.J.; Kück, U. The novel ER membrane protein PRO41 is essential for sexual development in the filamentous fungus *Sordaria macrospora*. *Mol. Microbiol.* **2007**, *64*, 923–937. [\[CrossRef\]](#)
31. Odenbach, D.; Breth, B.; Thines, E.; Weber, R.W.S.; Anke, H.; Foster, A.J. The transcription factor Con7p is a central regulator of infection-related morphogenesis in the rice blast fungus *Magnaporthe grisea*. *Mol. Microbiol.* **2007**, *64*, 293–307. [\[CrossRef\]](#) [\[PubMed\]](#)
32. Copenhaver, G.P.; Kim, S.; Park, S.-Y.; Kim, K.S.; Rho, H.-S.; Chi, M.-H.; Choi, J.; Park, J.; Kong, S.; Park, J.; et al. Homeobox Transcription Factors Are Required for Conidiation and Appressorium Development in the Rice Blast Fungus *Magnaporthe oryzae*. *PLoS Genet.* **2009**, *5*, e1000757. [\[CrossRef\]](#)
33. Yang, J.; Zhao, X.; Sun, J.; Kang, Z.; Ding, S.; Xu, J.-R.; Peng, Y.-L. A novel protein Com1 is required for normal conidium morphology and full virulence in *Magnaporthe oryzae*. *Mol. Plant-Microbe Interact.* **2010**, *23*, 112–123. [\[CrossRef\]](#) [\[PubMed\]](#)
34. Guo, M.; Guo, W.; Chen, Y.; Dong, S.; Zhang, X.; Zhang, H.; Song, W.; Wang, W.; Wang, Q.; Lv, R.; et al. The basic leucine zipper transcription factor Moatf1 mediates oxidative stress responses and is necessary for full virulence of the rice blast fungus *Magnaporthe oryzae*. *Mol. Plant-Microbe Interact.* **2010**, *23*, 1053–1068. [\[CrossRef\]](#) [\[PubMed\]](#)
35. Zhou, X.; Liu, W.; Wang, C.; Xu, Q.; Wang, Y.; Ding, S.; Xu, J.R. A MADS-box transcription factor MoMcm1 is required for male fertility, microconidium production and virulence in *Magnaporthe oryzae*. *Mol. Microbiol.* **2011**, *80*, 33–53. [\[CrossRef\]](#)
36. Koo, S.C.; Moon, B.C.; Kim, J.K.; Kim, C.Y.; Sung, S.J.; Kim, M.C.; Cho, M.J.; Cheong, Y.H. OsBWMK1 mediates SA-dependent defense responses by activating the transcription factor OsWRKY33. *Biochem. Biophys. Res. Commun.* **2009**, *387*, 365–370. [\[CrossRef\]](#)
37. Kim, S.; Kim, C.-Y.; Park, S.-Y.; Kim, K.-T.; Jeon, J.; Chung, H.; Choi, G.; Kwon, S.; Choi, J.; Jeon, J. Two nuclear effectors of the rice blast fungus modulate host immunity via transcriptional reprogramming. *Nat. Commun.* **2020**, *11*, 5845. [\[CrossRef\]](#)
38. Chen, S.; Songkumarn, P.; Venu, R.; Gowda, M.; Bellizzi, M.; Hu, J.; Liu, W.; Ebbole, D.; Meyers, B.; Mitchell, T. Identification and characterization of in planta-expressed secreted effector proteins from *Magnaporthe oryzae* that induce cell death in rice. *Mol. Plant-Microbe Interact.* **2013**, *26*, 191–202. [\[CrossRef\]](#)



39. Guo, X.; Zhong, D.; Xie, W.; He, Y.; Zheng, Y.; Lin, Y.; Chen, Z.; Han, Y.; Tian, D.; Liu, W.; et al. Functional Identification of Novel Cell Death-inducing Effector Proteins from *Magnaporthe oryzae*. *Rice* **2019**, *12*, 59. [[CrossRef](#)]
40. Xu, J.-R.; Hamer, J.E. MAP kinase and cAMP signaling regulate infection structure formation and pathogenic growth in the rice blast fungus *Magnaporthe grisea*. *Genes Dev.* **1996**, *10*, 2696–2706. [[CrossRef](#)]
41. Osés-Ruiz, M.; Cruz-Mireles, N.; Martin-Urdiroz, M.; Soanes, D.M.; Eseola, A.B.; Tang, B.; Derbyshire, P.; Nielsen, M.; Cheema, J.; Were, V.; et al. Appressorium-mediated plant infection by *Magnaporthe oryzae* is regulated by a Pmk1-dependent hierarchical transcriptional network. *Nat. Microbiol.* **2021**, *6*, 1383–1397. [[CrossRef](#)] [[PubMed](#)]
42. Sakulkoo, W.; Osés-Ruiz, M.; Oliveira Garcia, E.; Soanes, D.M.; Littlejohn, G.R.; Hacker, C.; Correia, A.; Valent, B.; Talbot, N.J. A single fungal MAP kinase controls plant cell-to-cell invasion by the rice blast fungus. *Science* **2018**, *359*, 1399–1403. [[CrossRef](#)] [[PubMed](#)]
43. Lu, K.; Chen, R.; Yang, Y.; Xu, H.; Jiang, J.; Li, L. Involvement of the cell wall integrity pathway in signal recognition, cell wall biosynthesis, and virulence in *Magnaporthe oryzae*. *Mol. Plant-Microbe Interact.* **2023**, *36*, 608–622. [[CrossRef](#)] [[PubMed](#)]
44. Cai, Y.Y.; Wang, J.Y.; Wu, X.Y.; Liang, S.; Zhu, X.M.; Li, L.; Lu, J.P.; Liu, X.H.; Lin, F.C. MoOpy2 is essential for fungal development, pathogenicity, and autophagy in *Magnaporthe oryzae*. *Environ. Microbiol.* **2022**, *24*, 1653–1671. [[CrossRef](#)] [[PubMed](#)]
45. Ryder, L.S.; Dagdas, Y.F.; Kershaw, M.J.; Venkataraman, C.; Madzvamuse, A.; Yan, X.; Cruz-Mireles, N.; Soanes, D.M.; Osés-Ruiz, M.; Styles, V.; et al. A sensor kinase controls turgor-driven plant infection by the rice blast fungus. *Nature* **2019**, *574*, 423–427. [[CrossRef](#)]
46. Zhang, H.; Liu, K.; Zhang, X.; Song, W.; Zhao, Q.; Dong, Y.; Guo, M.; Zheng, X.; Zhang, Z. A two-component histidine kinase, MoSLN1, is required for cell wall integrity and pathogenicity of the rice blast fungus, *Magnaporthe oryzae*. *Curr. Genet.* **2010**, *56*, 517–528. [[CrossRef](#)]
47. Aron, O.; Wang, M.; Lin, L.; Batool, W.; Lin, B.; Shabbir, A.; Wang, Z.; Tang, W. MoGLN2 is important for vegetative growth, conidiogenesis, maintenance of cell wall integrity and pathogenesis of *Magnaporthe oryzae*. *J. Fungi* **2021**, *7*, 463. [[CrossRef](#)]
48. Seiboth, B.; Pakdaman, B.S.; Hartl, L.; Kubicek, C.P. Lactose metabolism in filamentous fungi: How to deal with an unknown substrate. *Fungal Biol. Rev.* **2007**, *21*, 42–48. [[CrossRef](#)]
49. Chroumpi, T.; Mäkelä, M.R.; de Vries, R.P. Engineering of primary carbon metabolism in filamentous fungi. *Biotechnol. Adv.* **2020**, *43*, 107551. [[CrossRef](#)]
50. Kong, L.-A.; Yang, J.; Li, G.-T.; Qi, L.-L.; Zhang, Y.-J.; Wang, C.-F.; Zhao, W.-S.; Xu, J.-R.; Peng, Y.-L. Different chitin synthase genes are required for various developmental and plant infection processes in the rice blast fungus *Magnaporthe oryzae*. *PLoS Pathog.* **2012**, *8*, e1002526. [[CrossRef](#)]
51. Pan, B.-Y.; Li, G.-Y.; Wu, Y.; Zhou, Z.-S.; Zhou, M.; Li, C.J. Glucose utilization in the regulation of chitin synthesis in brown planthopper. *J. Insect Sci.* **2019**, *19*, 3. [[CrossRef](#)] [[PubMed](#)]
52. Yang, S.; Zou, Z.; Xin, T.; Cai, S.; Wang, X.; Zhang, H.; Zhong, L.; Xia, B. Knockdown of hexokinase in *Diaphorina citri* Kuwayama (Hemiptera: Liviidae) by RNAi inhibits chitin synthesis and leads to abnormal phenotypes. *Pest Manag. Sci.* **2022**, *78*, 4303–4313. [[CrossRef](#)] [[PubMed](#)]
53. Zhang, S.; Zhang, Y.; Zou, H.; Li, X.; Zou, H.; Wang, Z.; Zou, C. FDP-Na-induced enhancement of glycolysis impacts larval growth and development and chitin biosynthesis in fall webworm, *Hyphantria cunea* (Lepidoptera: Arctiidae). *Pestic. Biochem. Physiol.* **2023**, *195*, 105560. [[CrossRef](#)] [[PubMed](#)]

**Disclaimer/Publisher’s Note:** The statements, opinions and data contained in all publications are solely those of the individual author(s) and contributor(s) and not of MDPI and/or the editor(s). MDPI and/or the editor(s) disclaim responsibility for any injury to people or property resulting from any ideas, methods, instructions or products referred to in the content.